Cloud Soft Leather Shoes For All Day Pain Free Walking
wywpoo
Open

RESEARCH ARTICLE | ECOLOGY

Rapid coral bleaching recovery via symbiont transfer from healthy corals

DANIEL S. COLLINS, JANA SIPKOVA, NATHANIEL R. MOLLICA, THOMAS ROLANDER, [...], AND STEPHEN R. PALUMBI +4 authors Authors Info & Affiliations

SCIENCE ADVANCES • 14 Oct 2026 • Vol 12, Issue 42 • DOI: 10.1126/sciadv.aeh1580

Abstract

Coral bleaching, the temperature-induced loss of dinoflagellate symbionts, is a major driver of global coral reef decline. Although corals can regain symbionts through repopulation of residual symbionts or via environmental acquisition, these processes are often too slow to prevent coral mortality. Mechanisms that enable rapid and effective symbiont reintroduction leading to full recovery remain largely unknown. Here, we demonstrate coral bleaching recovery through contact-mediated transfer of symbionts from healthy corals using small coral fragments. We show that symbiont transfer is rapid, occurring over days to weeks, and highly efficient, with only brief physical contact with healthy corals required. A single week of contact, and in some cases as few as 3 days, provides sufficient symbionts to initiate sustained and full self-recovery. By 1 week, symbiont population doubling time is approximately 4 days, up to an order of magnitude faster than most recovery times for corals in the field. We identify tissue fusion as the mechanism enabling directional symbiont transfer from healthy to bleached coral tissue. As a result, contact-dependent recovery is restricted to corals of the same genet, whereas heterologous genet pairings trigger antagonistic interactions. However, symbiont transfer via polyp uptake occurs immediately upon contact in both same-genet and mixed-genet pairings, revealing an additional, slower pathway for symbiont transfer that is insufficient on its own to support colony recovery. Collectively, these findings reveal a previously unrecognized natural process for efficiently reintroducing symbionts to bleached corals, providing a foundation for research into potential recovery interventions.

SIGN UP FOR THE AWARD-WINNING *SCIENCE*ADVISER NEWSLETTER
The latest news, commentary, and research, free to your inbox daily
SIGN UP >

INTRODUCTION

Coral reefs are experiencing global declines as rising seawater temperatures cause widespread bleaching (1). Thermal stress can induce coral bleaching by disrupting the symbiotic relationship between corals and their dinoflagellate symbionts (Symbiodiniaceae), triggering symbiont expulsion from coral tissues (2). These symbionts supply most of the coral's nutrients through photosynthesis, and without symbionts, corals are vulnerable to starvation and overgrowth by external filamentous algae on the coral surface, often resulting in mortality (1, 3–6). In some cases, however, bleached corals can recover and return to a healthy state once heat stress subsides (7–9), yet there have been very few studies on the processes that enable this recovery (7–11). Recovery can occur through the repopulation of remaining symbionts in partially bleached corals. Alternatively, bleached corals can recover through the acquisition of symbionts expelled at a slow rate by healthy corals (11–15). Careful search of coral habitats has shown that indeed symbionts are present in reef sediments and the water column, but occur at abundances several orders of magnitude lower than in coral tissues (16–18), potentially limiting recovery through environmental acquisition. Both of these natural recovery pathways are typically slow, occurring over months and contributing to the high mortality rates observed during severe bleaching events (6, 7, 19).

There is an ongoing, urgent race for solutions to mitigate the catastrophic loss of coral due to bleaching. With widespread impacts from four global bleaching events occurring in 1998, 2010, 2015 to 2016, and 2023 to 2025, and predictions of mass coral bleaching occurring annually by 2080, coral reefs are approaching tipping points of collapse (20–22). Currently, most research is focused on understanding the heat tolerance of corals and their symbionts, and harnessing heat tolerance for coral conservation and restoration. Recent approaches include acclimatization, assisted evolution, genetic engineering, selective breeding, and manipulation of the coral holobiont through the introduction of probiotics, microbiome transplants, and heat-evolved symbionts (23–30). Other interventions aimed at reducing bleaching and its impacts include shading, coral transplantation, assisted gene flow, larval seeding, and coral nurseries (31–35). However, these solutions are largely preventative, designed to limit the effects of coral bleaching before or during thermal stress. While bleaching recovery mechanisms have been studied at the organismal and molecular scale (8, 36–39), comparatively little attention has been given to solutions for recovering corals that are already bleached, in part due to their typically low survival rate. Moreover, natural processes for rapidly reintroducing symbionts and enabling recovery remain largely unknown. Yet, many reefs can have localized bleaching where healthy colonies with dense symbiont populations can persist adjacent to bleached colonies, providing a natural reservoir of symbionts that could potentially be leveraged for recovery (40). This raises the question of whether healthy, unbleached corals could promote the recovery of bleached corals through direct symbiont reintroduction.

Here, we report rapid coral bleaching recovery through direct contact with healthy corals. We show that contact between healthy and bleached coral fragment (*Pocillopora damicornis*) leads to rapid symbiont transfer, resulting in full recovery within weeks. In contrast, bleached corals that are not in contact with healthy corals experience extensive algal overgrowth and mortality. Symbiont transfer initiates at the contact interface and subsequently spreads throughout the bleached fragment. Notably, just 1 week of contact provides sufficient symbionts for the bleached coral to fully recover even after separation from the healthy coral. In same-genet pairings, separation revealed tissue rips in identical locations on both healthy and bleached corals, and an accumulation of symbionts in the bleached tissue, indicating that directional symbiont transfer is facilitated by rapid tissue fusion. We find that this recovery is restricted to corals of the same genet, whereas pairings between different genets trigger antagonistic interactions, with the healthy coral overtaking the bleached fragment. In addition, we identify a secondary, less efficient mechanism of transfer in which symbionts are expelled from the healthy coral onto the bleached coral before fusion, a process observed in both same-genet and mixed-genet pairings. Collectively, our experimental results demonstrate that healthy corals can rapidly recover bleached corals through direct symbiont delivery.

RESULTS

Direct contact with healthy coral drives full recovery of bleached coral

To test the hypothesis that bleached corals can be recovered through direct contact with a healthy coral, we placed bleached coral fragments (1 to 1.5 cm in length) of *P. damicornis* in contact with healthy fragments of the same genet (i.e., a clonal genotype). All bleached coral in direct contact with healthy coral ($n = 5$) achieved complete recovery within 8 weeks. The bleached corals were rapidly recolonized by symbionts from the healthy coral (Fig. 1A). Symbiont repopulation was first observed at the contact interface and progressively expanded throughout the bleached coral, resulting in full recovery. Recovery was consistently observed across all bleached corals in contact with healthy corals. To determine whether contact was required for recovery, bleached fragments were positioned 5 to 7 mm away from healthy coral fragments ($n = 5$). These bleached corals held millimeters from healthy corals remained fully bleached for several weeks, followed by severe overgrowth of filamentous red and green algae and diatoms, and subsequent tissue necrosis and polyp mortality (Fig. 1B). We repeated the experiment with relatively larger coral fragments (2 to 3 cm in length) and obtained similar results for both contacting and noncontacting bleached corals (fig. S1).

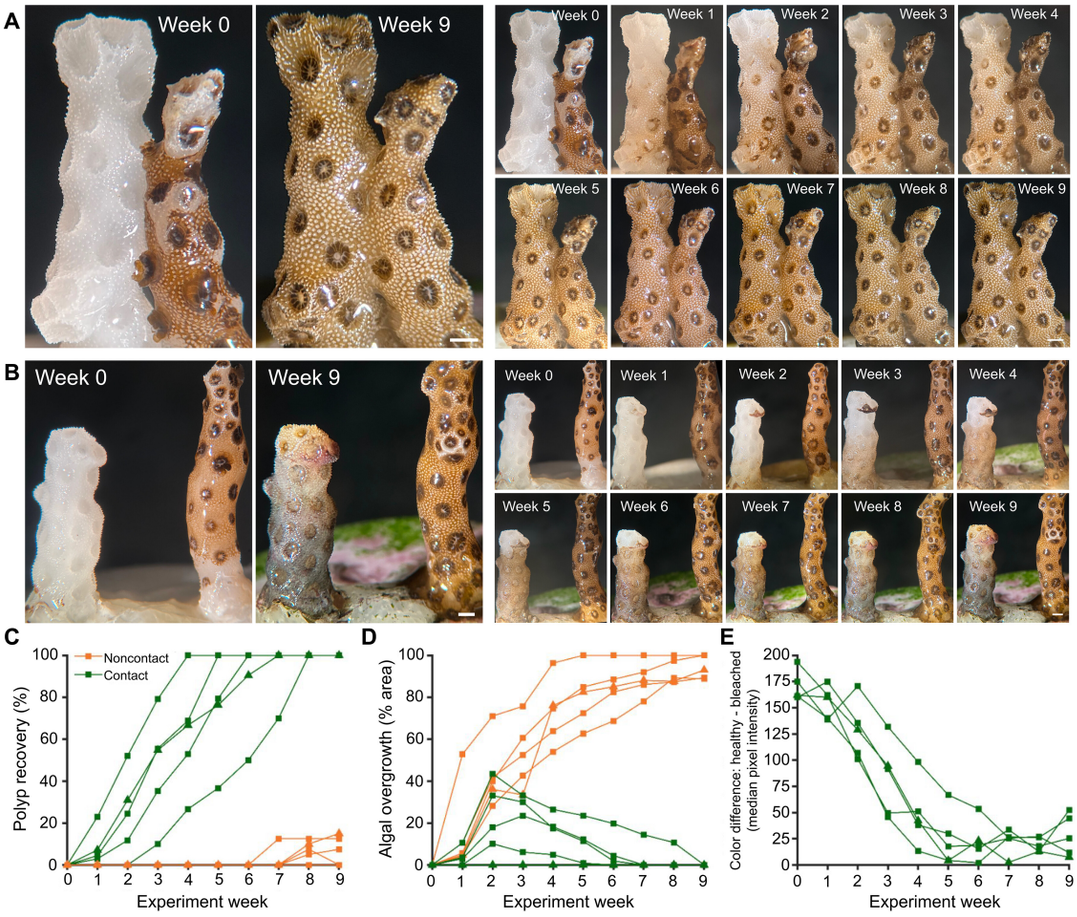

Fig. 1. Coral bleaching recovery through contact with healthy coral.
(**A**) Example stereoscopic images of a bleached and healthy coral fragment (*P. damicornis*) in direct contact, showing weekly progression of coral bleaching recovery from week 0 to week 9. Scale bars, 1 mm. (**B**) Example stereoscopic images of a bleached and healthy coral fragment (*P. damicornis*) without contact, showing weekly progression from week 0 to week 9 of external algal overgrowth composed of filamentous red and green algae and diatoms. Overgrowth is characterized by a greenish hue and typically initiates from the base, leading to mortality and minimal recovery. Scale bars, 1 mm. (**C**) Polyp recovery of bleached coral fragments with and without contact with healthy coral fragments from week 0 to week 9. Polyp recovery was normalized to the total number of polyps per fragment, $n = 5$ (contact) and $n = 5$ (noncontact). (**D**) Area of algal overgrowth on bleached coral fragments with and without contact with healthy coral fragments from week 0 to week 9. Algal overgrowth area was normalized to fragment size, $n = 5$ (contact) and $n = 5$ (noncontact). (**E**) Differences in median pixel color of bleached coral fragments in contact with healthy coral fragments from week 0 to week 9, $n = 5$. Coral fragments shown in (A) and (B) are represented by triangles. Scale bars, 1 mm.

All bleached corals in contact with healthy corals achieved 100% polyp recovery after 8 weeks, with one fragment reaching full polyp recovery after only 4 weeks (Fig. 1C). In addition, by the end of the experiment, recovered bleached fragments had a greater number of polyps than initially present, indicating a transition into active growth involving new tissue, skeletal growth, and polyp formation (fig. S2). For the noncontacting bleached corals, four of five fragments showed minimal polyp recovery (5 to 20%) at the branching tip of the fragment during the final 3 weeks of the experiment (Fig. 1C). This limited recovery likely arose from either acquisition of expelled symbionts from nearby healthy corals or repopulation of residual symbionts in the tissue (*41*). At the end of 9 weeks, two of the isolated bleached fragments were fully overgrown by algae and died, and the other three exhibited algal overgrowth covering ≥87% of the fragment, outpacing symbiont repopulation (Fig. 1D). In contrast, the contacting pairs exhibited limited algal overgrowth, which peaked by the second week. By the end of the experiment, no algal overgrowth was observed on any of these contacting fragments because new tissue had grown over areas covered in algae (Fig. 1D). Analysis of the images collected throughout the experiment revealed that the median pixel color values of bleached corals progressively approached those of healthy corals, with minimal differences by the final weeks, indicating recovery of pigmentation (Fig. 1E).

The corals were re-evaluated at week 20, and previously bleached fragments in contact with healthy corals showed extensive additional polyp growth and produced new branches similar to those of their healthy counterparts. (fig. S3). In contrast, recovery in noncontacting corals had further declined relative to week 9, due to algal overgrowth and tissue death preventing further recovery (Fig. 1, C to E, and fig. S3).

Brief contact with healthy coral initiates self-sustained recovery of bleached coral

To test whether sustained physical contact with a healthy coral was required for complete bleaching recovery, we separated bleached corals from healthy corals after varying contact durations ranging from 1 day to 3 weeks (see Materials and Methods). All bleached corals with 1 week or longer con-tact, and one coral with 5 days of contact, achieved complete polyp recovery within 7 weeks (n = 6) (Fig. 2, A, B, and D). These experiments showed that 1 week of contact provides sufficient symbiont transfer for bleached fragments to fully recover independently. At even shorter contact intervals, we observed that all fragments in contact with healthy coral for ⩾3 days exhibited symbiont transfer and visible signs of recovery at separation (n = 10) (fig. S4), but were ultimately covered by algae (Fig. 2C). By contrast, a limited sample of bleached corals in contact for only 1 day (n = 2) showed no recovery at separation.

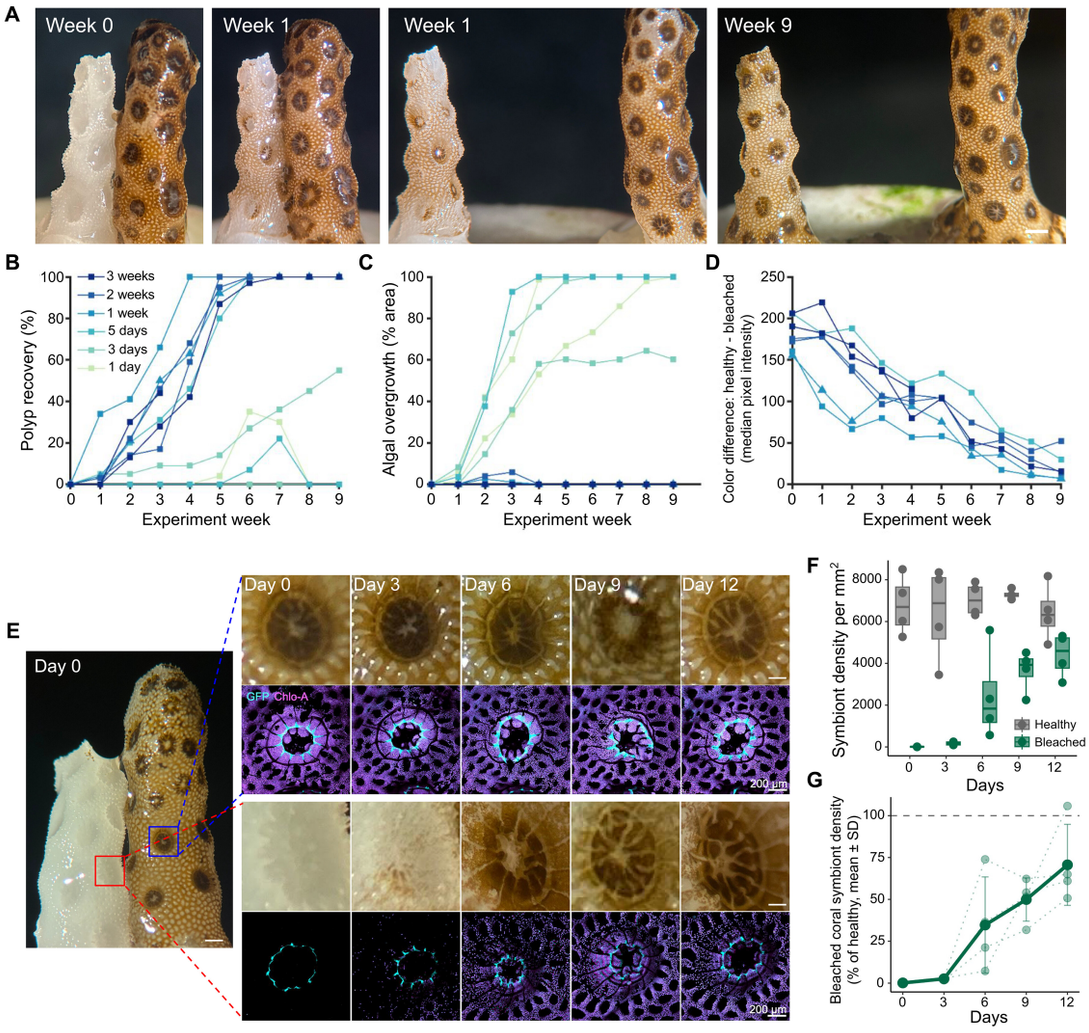

Fig. 2. Rapid symbiont transfer facilitates recovery.
(**A**) Example stereoscopic images of a bleached coral fragment in contact with a healthy coral fragment at weeks 0 and 1, followed by separation at week 1 and full recovery by week 9. Scale bars, 1 mm. (**B**) Polyp recovery of bleached coral fragments following contact with and subsequent separation from healthy coral fragments from week 0 to week 9. Polyp recovery was normalized to the total number of polyps per fragment, n = 2 (per condition). (**C**) Area of algal overgrowth on

Expand for more

Monitoring recovery after separation allowed us to track key aspects of the recovery process. In previous experiments with continuous contact (Fig. 1), increases in symbiont density in bleached corals could have resulted from both continued transfer from the healthy coral and replication of symbionts within the bleached fragment. By contrast, in separated corals, all subsequent increases in symbiont density must result from symbiont replication. In these separation experiments, bleached corals that were in contact with a healthy coral for a week or longer achieved full recovery within 7 weeks, matching the recovery rate observed in the continuously contacting corals, with some separated fragments exceeding this rate (Figs. 1C and 2B). This similar recovery rate following separation suggests that full recovery is largely driven by symbiont replication within the recipient bleached coral.

Rapid directional symbiont transfer from healthy to bleached coral

We monitored bleached and healthy polyps using laser scanning confocal microscopy (LSCM) every 3 days over a 12-day period, to better understand the process of symbiont transfer. Symbionts were visible in the Chlo-*a* channel, whereas corals produced a chromoprotein visible in the GFP channel (Fig. 2, E and F). Symbiont density measurements were performed on polyps, which contain higher symbiont densities than the coenosarc (the interpolyp tissue). On day 0, bleached polyps exhibited a mean symbiont density of 7 cells/mm^2, with one fragment containing no detectable symbionts. The healthy polyps exhibited a mean symbiont density of more than 6700 cells/mm^2, indicating that the bleached corals had lost 99.9 to 100% of their symbionts (Fig. 2, E and F). Thus, substantial presence of symbionts reflects reintroduction from external sources, not repopulation of remnant symbionts. By day 3, symbionts were observed in polyps of bleached fragments (Fig. 2, F and G); however, substantial recovery in symbiont density began after day 3 (Fig. 2, F and G). Symbiont density continued increasing through day 12, with previously bleached polyps reaching 70.6 ± 24.2% (mean ± SD) of the density of adjacent healthy polyps per coral pair (n = 4). The symbiont doubling time in these contact experiments is 18.3 ± 5.8 hours (mean ± SD) in the first 6 days and 4.13 ± 1.7 days (mean ± SD) in the following 6 days, reflecting immediate import of symbionts followed by steady, rapid replication thereafter (table S1 and fig. S5).

Microscopic inspection during recovery revealed that symbionts initially transferred at the contact interface subsequently spread throughout the fragment until full recovery (Fig. 2E). In fragments separated after 1 week, symbiont densities did not visibly differ from the previously contacting side and the opposite side of the fragment, indicating that the rapid increase in symbiont density in the bleached fragment was additionally associated with intracolony transport (Fig. 2A).

Coral bleaching recovery requires same-genet pairing

Experiments shown in Figs. 1 and 2 were performed using coral fragments from a single genet (genotype R). To assess whether this recovery pattern occurred in other genets, we repeated the contact versus no contact experiment using a different genet (genotype G; n = 3 contact, n = 3 non-contact) and observed the same robust and reproducible bleaching recovery (fig. S6). We then tested bleaching recovery across genets by pairing bleached corals of genotype G with healthy corals of genotype R (n = 3) and vice versa (n = 3).

We then tested bleaching recovery across genets by pairing bleached corals of genotype G with healthy corals of genotype R (n = 3) and vice versa (n = 3). In contrast to R-R and G-G pairings, within hours of mixed pairings, we observed mesenterial filaments at the interface between corals (Fig. 3A). These filaments, ejected from coral polyps and lined with stinging nematocysts, suggest antagonistic interactions consistent with biological warfare (*42*). Filaments remained extended at the contact interface for several weeks and were absent in same-genet contacts. We observed limited symbiont transfer in bleached polyps, consistent with symbionts expelled by adjacent healthy corals and subsequently acquired by nearby bleached polyps (*12*, *43*). However, this transfer did not result in large-scale recovery thereafter (fig. S7). Instead, all bleached fragments in mixed genotype pairing were extensively overgrown by healthy coral, with four of six bleached fragments fully overgrown at 9 weeks (Fig. 3, B and C). Overgrowth likely resulted from the weakened state of bleached fragments due to heat stress and symbiont loss, reducing energy and competitive defenses. Regions not overgrown by healthy coral were instead overgrown by algae. Across the experiment, none of the bleached fragments showed signs of recovery (Fig. 3D).

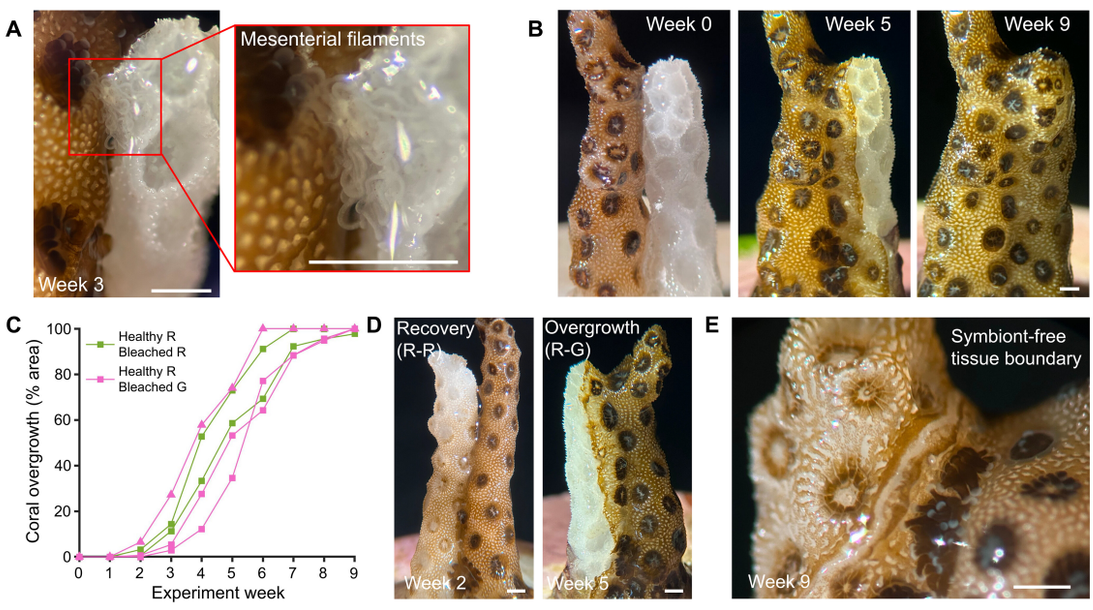

Fig. 3. Bleaching recovery requires same-genet pairing.
(**A**) Example stereoscopic image of mesenterial filaments deployed at the contact interface between healthy and bleached coral fragments; the bleached fragment is genotype G and the healthy fragment is genotype R. Scale bars, 1 mm. (**B**) Example stereoscopic image of a bleached and healthy coral fragment of different genets in contact, showing weekly progression of competitive overgrowth from week 0 to week 9; the bleached fragment is genotype G and the healthy fragment is genotype R. Scale bar, 1 mm. (**C**) Area of overtake of bleached coral fragments by healthy coral fragments in different-genet pairings. Overtake area was normalized to fragment size, $n = 3$ (R-G) and $n = 3$ (G-R). Excludes one pair (healthy G + bleached R) that did not maintain contact. Coral fragment shown in (B) is represented by triangles. (**D**) Example stereoscopic images of recovery in same-genet pairings at week 2 (left; genotype R) with overgrowth in different-genet pairings at week 5 (right; bleached fragment genotype R, healthy fragment genotype G). Scale bars, 1 mm. (**E**) Example stereoscopic images of symbiont-free tissue boundary between healthy coral fragments of genotype R (left) and genotype G (right). Scale bar, 1 mm.

To explore mixed-genet interactions without bleached fragments, we paired healthy fragments from both genets ($n = 4$) and observed mesenterial filaments and a clear tissue boundary, consistent with previous descriptions of *P. damicornis* (*44*) (Fig. 3E). At the contact interface, we observed a zone of symbiont-free tissue, indicating absence of symbiont exchange between genets. This explains the lack of mass symbiont transfer in bleached-healthy mixed-genet pairings.

Together, these results suggest that coral bleaching recovery we describe here is limited to corals of the same genet. Although symbiont transfer via polyp uptake occurred in mixed-genet pairings, it was insufficient to support fragment-wide recovery. Thus, the bleaching recovery observed in Figs. 1 and 2 is not due merely to proximity or physical contact, but involves active, contact-mediated symbiont transfer between a healthy and bleached coral fragment of the same genet.

Tissue fusion enables direct symbiont transfer driving bleaching recovery

To gain insight into the mechanism of symbiont transfer, we tracked the spatiotemporal spread of symbionts from healthy to bleached corals using larger coral fragments (2 to 3 cm) in both R-R and G-G pairings ($n = 3$ per treatment). We observed that symbiont transfer from healthy to bleached corals initiated at localized points of contact between fragments rather than uniformly across the entire contact interface. Initial transfer sites occurred at different positions along the bleached fragment among replicates (Fig. 4, A to C, and fig. S8). Following initial transfer, symbionts spread outward from the transfer site, progressively recolonizing the entire bleached fragment. Recolonization proceeded top-down when transfer initiated at the fragment tip, bottom-up when transfer initiated at the base, and bidirectionally when transfer was initiated at the midpoint (Fig. 4, A to C, and fig. S8). In all fragments examined ($n = 6$), recolonization expanded from localized transfer sites and spread throughout the fragment. One fragment exhibited two transfer sites, at the tip and midpoint of the fragment, from which recolonization proceeded simultaneously from both transfer sites (fig. S8A). The directional pattern of symbiont recolonization observed at the fragment level was also evident within individual polyps (fig. S9). In fragments exhibiting top-down recovery, symbionts first appeared in the upper tentacles of individual polyps before spreading to lower tentacles (fig. S9A). Conversely, in fragments exhibiting bottom-up recovery, symbionts first appeared in lower tentacles and subsequently spread to the upper tentacles (fig. S9B). These observations show that symbiont transfer initiates at localized contact sites, followed by directional, fragment-wide recolonization.

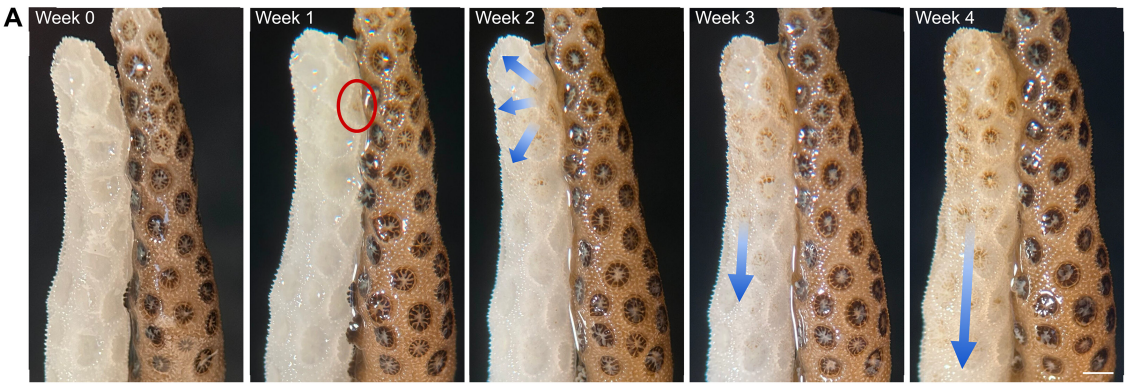

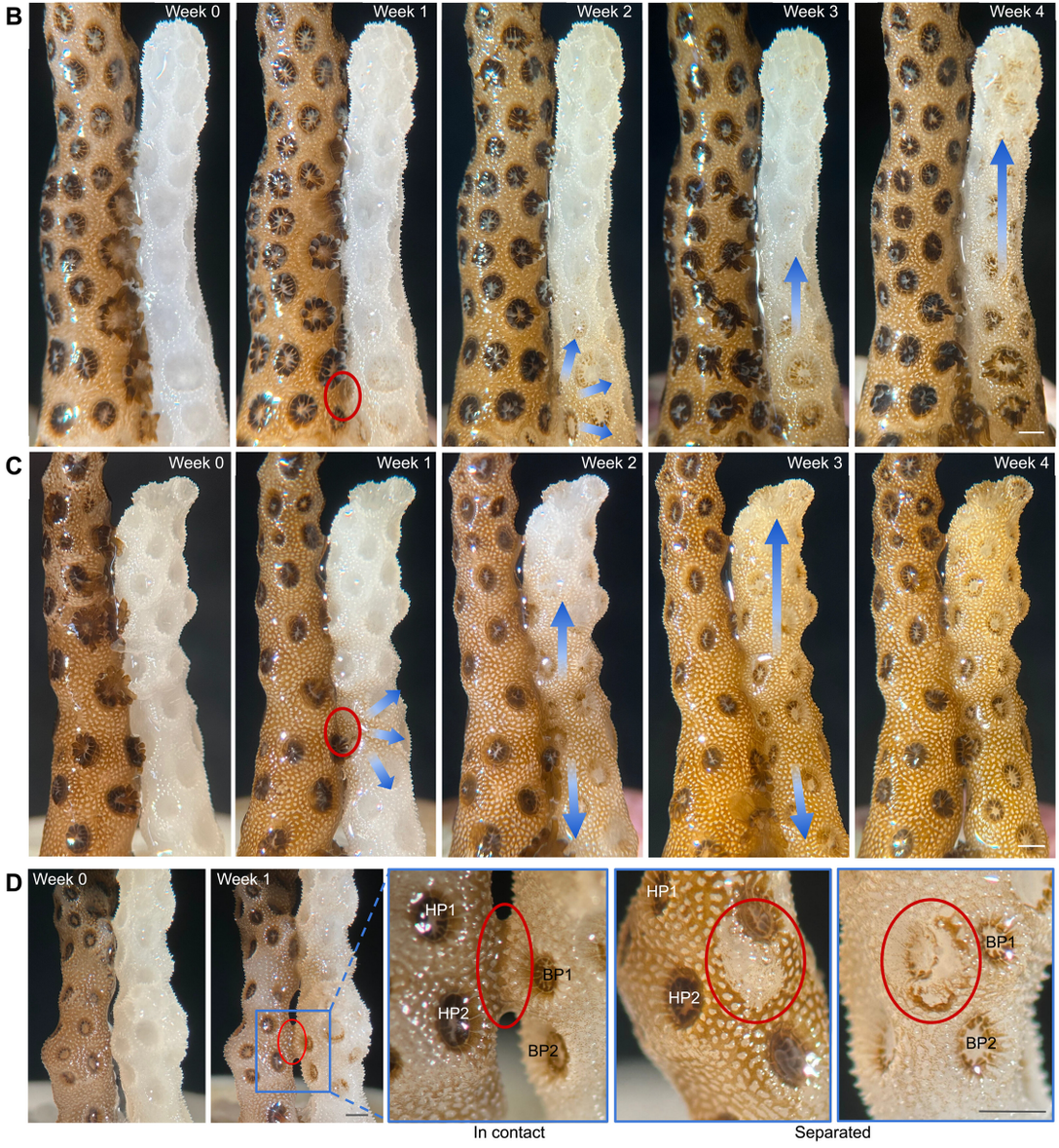

Fig. 4. Directional symbiont spread during recovery originates from localized tissue fusion sites.
(**A** to **C**) Example stereoscopic images showing symbiont transfer initiating from tissue bridges (red ovals) located at the fragment tip (A), base (B), or midpoint (C), resulting in top-down, bottom-up, or bidirectional recolonization of the bleached fragment, respectively (blue arrows). Images show recovery from week 0 to week 4. Scale bars, 1 mm. (**D**) Example stereoscopic images showing symbiont transfer initiating from a tissue bridge (red oval) near the base of the bleached coral, resulting in bottom-up recolonization (blue arrows). After 2 weeks of contact, the fragments were separated, revealing corresponding tissue rips at the site of initial symbiont transfer on both the healthy (left) and bleached (right) corals. The paired tissue rips are indicated by red ovals. Labeled polyps on each coral provide reference points for comparing orientation before and after separation. Scale bars, 1 mm.

The pattern of symbiont spread at local contact points and its radial propagation throughout the fragment, coupled with its restriction to same-genet pairings, suggest that this contact-mediated transfer involves same-genet tissue recognition and fusion. This mechanism is consistent with observations of fusion between same-genet corals and formation of continuous tissue across contact interfaces (*44*–*49*). To test this hypothesis, we set up additional contacting pairs (n = 12), monitored recovery over several weeks, and identified the focal points of symbiont reintroduction before separating the two fragments.

Separation consistently revealed paired tissue rips exposing the skeleton at identical locations on both healthy and bleached corals, corresponding to the sites of initial symbiont spread (Fig. 4D, fig. S10, and movie S1). These localized, paired rips indicate the presence of tissue bridges between fragments at the point of symbiont transfer, which were torn upon separation. Across all replicates, the tissue rips were confined to the transfer sites; fragments exhibited no additional damage beyond these rips. In cases where two distinct transfer sites were observed, two corresponding sets of matching tissue rips were present on both fragments (fig. S10C). To test whether tissue rips resulted from mechanical damage during contact and separation, we set up contacting pairs for 1 day before separation (n = 6). No ripping was observed, indicating that the rips are not attributable to contact alone but consistent with disruption of fused tissue (fig. S11).

To resolve the early dynamics of symbiont transfer, we monitored contacting pairs over the first 72 hours of contact (n = 6). Within hours, small numbers of symbionts accumulated in bleached polyps, consistent with the limited polyp uptake observed in mixed-genet pairings (fig. S12A). Between 36

and 60 hours after contact, symbiont transfer rapidly increased at localized sites along the contact interface (fig. S12B). Symbionts subsequently spread from the transfer sites to adjacent bleached polyps (fig. S12B). Separation of the fragments at 72 hours revealed matching tissue tears at the transfer sites, with no additional visible tissue damage (fig. S12C). Together, these observations suggest that rapid mass transfer begins approximately 36 to 60 hours after contact, coinciding with localized tissue bridges formation between fragments, leading to directional symbiont spread that recolonizes the bleached fragment.

DISCUSSION

This study provides a repeatable demonstration of coral bleaching recovery through direct contact with same-genet, healthy, unbleached corals, resulting in complete recovery of bleached fragments in as little as 4 weeks. Thus, we document symbiont transfer from a healthy coral as a robust, natural mechanism for rapid symbiont reintroduction to a bleached coral mediated by physical contact. In the absence of contact with healthy coral, bleached corals exhibited high mortality rates similar to those commonly observed on bleached reefs. We also found that, following rapid mass transfer, symbionts were distributed throughout the fragment, emphasizing the role of coral's gastrovascular circulation in recovery. These results advance our understanding of the physiological and cellular processes that enable coral recovery following bleaching.

Recent work has explored the use of healthy corals as donors of heat-tolerant symbionts to bleached corals, with transfer occurring through the water column (*19*, *41*). However, this process resulted in limited uptake of heat-tolerant symbionts by bleached corals: after 55 days of exposure, only 5 of 45 recipient fragments contained even low levels (⩽0.06%) of the donor symbiont (*41*). Consistent with these findings, we observed that even when bleached corals were positioned just a few millimeters from healthy corals, symbiont transfer and environmental acquisition remained limited. Expanding on this work on recovery of original symbiont populations, contact-dependent symbiont transfer could also provide an efficient means of replacing original symbionts with naturally occurring heat-tolerant symbionts (e.g., *Durusdinium*) or even heat-evolved symbionts (*30*, *50*, *51*), promoting rapid recovery while potentially enhancing thermal tolerance.

Our surveys indicate a symbiont doubling rate of approximately 4 days within bleached fragments during the second week of contact with healthy corals, which is substantially faster than the recovery rate of bleached corals in other studies. For example, on the Great Barrier Reef, symbiont loads in *Acropora* corals were documented to double over 3 months during bleaching recovery (*52*). In Samoa, symbionts in recovering *Montipora* corals doubled within 16 to 24 days, although a subset showed faster rates of 6 to 8 days (*14*). Rapid proliferation of newly acquired symbionts has also been documented in other cnidarian hosts, including *Aiptasia*, consistent with rapid symbiont expansion during early colonization of unpopulated host tissue (*53*). Slow recovery in corals may reflect host-imposed regulation of symbiont growth via nutrient or space constraints (*54*, *55*), which, in established coral colonies, limits proliferation through restricted host supply of nutrients, including nitrate and phosphate (*56*). Notably, the symbiont doubling rates observed here are consistent with reduced host-imposed constraints during the early stages of repopulation in bleached corals. The mechanisms by which transferred symbionts increase replication in bleached corals remain unclear, but the accelerated recovery rates observed in our study may reflect the absence of prior thermal stress in transferred symbionts. This possibility is supported by experiments showing that heat stress can impair symbiont replication and reduce metabolic support to the host (*57*–*59*). In addition, given the central role of host regulation of nutrient availability in symbiont population growth (*54*, *56*), nutrient transfer between healthy and bleached corals may have occurred during symbiont transfer and could therefore have contributed to rapid population expansion (*60*). Further work is needed to better understand these dynamics.

Symbiont transfer from healthy to bleached corals began at points of contact but spread rapidly throughout the entire fragment, suggesting transport through the gastrovascular network followed by proliferation within recipient tissues. Such rapid symbiont transport has been documented during new tissue growth (*61*). Similarly, when *Montipora* colonies were overturned, pale bottom tissues exhibited a rapid threefold increase in symbiont density, consistent with transport from the previously upper colony surface (*62*). In soft corals, ciliated gastrovascular canals transport symbiont-containing host cells throughout the colony, providing a mechanism for long-distance intracolonial movement (*63*–*66*). Evidence from *Aiptasia* supports a model in which colony-wide colonization involves both local proliferation and symbiont migration through host tissues (*67*). Many corals host distinct symbiont taxa in different regions of the colony, suggesting that intracolony transport is not unrestricted (68). Nevertheless, our data indicate that this intracolony transport during rapid symbiont population expansion may facilitate recovery and potentially drive colony-wide and reef-wide shifts in symbiont dominance following bleaching events (69–71). The cellular mechanisms of these processes in our system remain unresolved, and further work is needed to determine whether transferred symbionts are transported within host cells or as free-floating symbionts.

Fragment-wide recovery occurred only in same-genet pairings after tissue fusion. By contrast, heterologous pairings resulted in the rapid appearance of mesenterial filaments. Originally, mesenterial filaments were primarily viewed as defense mechanisms in interspecific competition (72, 73) but were then found to also be induced in some intraspecific interactions (74). These responses are governed by coral allorecognition systems that distinguish self from nonself tissues, triggering cellular responses that lead to tissue fusion or antagonistic rejection (75). Our findings indicate that in *P. damicornis*, this recognition system rapidly determines the outcome of contact between healthy and bleached fragments. If the genetic basis of this antagonistic response could be identified and modulated, it may be possible to promote fusion between corals of different genets, enabling mass symbiont transfer and recovery.

We also observed symbiont transfer from healthy to bleached corals within hours of contact, before fusion (fig. S12). This limited transfer likely occurred through the expulsion of symbionts from the healthy coral onto the bleached coral, with most symbionts accumulating in nearby bleached polyps. This pattern suggests that this symbiont uptake occurs via polyp ingestion followed by incorporation into gastrodermal cells, consistent with established mechanisms of environmental acquisition (76). Initial polyp uptake occurred in both same- and mixed-genet pairings, whereas the subsequent mass transfer was restricted to same-genet pairings, suggesting these represent mechanistically distinct modes of symbiont transfer. In mixed-genet pairings, the limited transfer was insufficient to promote recovery or prevent overgrowth by the healthy coral tissue, suggesting that the rapid symbiont doubling time we saw in same-genet interactions did not occur in this case. This cross-genet transfer indicates that the limitations of mass transfer and recovery observed in our experiments (Fig. 3) are driven by the coral host rather than the symbionts (fig. S7). Accordingly, enhancing the efficiency and scale of environmental acquisition could provide a strategy for reintroducing symbionts to bleached corals from healthy corals of different genets or even different species.

Our study reveals previously unrecognized dynamics both between coral hosts and their symbionts and among interacting corals. Open questions remain regarding the mechanisms responsible for rapid population expansion and the rapid colony transport we document, as well as the generality and scalability of our findings of coral bleaching recovery. In particular, future research should explore how consistently these recovery phenomena occur across coral species, symbiont taxa, and colony morphologies; evaluate the role of heterotrophic feeding in contact-mediated recovery; further investigate the mechanisms of symbiont transfer; and assess whether these transfer processes can be modified to facilitate universal symbiont transfer from healthy corals to bleached corals. The areal extent over which contact-mediated symbiont transfer can promote recovery within a colony remains unknown and may constrain recovery at larger scales. Extending these findings into ecologically relevant field contexts will be essential for evaluating coral bleaching recovery at the scale of natural coral reef systems.

Although the mechanism of coral bleaching recovery reported here is currently limited to same-genet pairing and sustained contact, our results establish a foundational framework for using healthy corals to rapidly reintroduce symbionts through contact and promote recovery in bleached corals. These findings may inspire a new class of responsive, postbleaching interventions aimed at accelerating coral bleaching recovery following bleaching events.

MATERIALS AND METHODS

Coral sampling and husbandry

Fragments of *P. damicornis* were derived from aquarium-maintained colonies originally obtained from aquarium suppliers; collection location and depth were not available. Colonies were maintained in aquaria at the Hopkins Marine Station, in Pacific Grove, CA, USA, for 3.5 years. Parental colonies before fragmentation were approximately 40 cm by 40 cm in size for each genotype. The two genotypes were distinguished by fluorescence under blue excitation light, used as a visual marker for genotype identification: genotype R fluoresced red and genotype G fluoresced green. The molecular basis of this variation was not investigated in this study. Corals were maintained in flow-through aquaria at temperatures ranging 27° to 28°C and fed a mixture of Restor Liquid Coral Tissue Nutritional Supplement, Zooplanktos-M (500 to 1000 μm), Reef Snow, and Reef Blizzard-XC (all from Brightwell Aquatics, Fort Payne, AL), at final concentrations of 100, 100, and 50 μl/liter, respectively. Small invertebrates present in the aquaria included snails, amphipods, *Xenia* octocorals, *Aiptasia*, small brooding sea stars, and annelids. These organisms were not detrimental to the corals or experimentally manipulated, and all treatments were maintained under identical conditions. The colonies hosted *Cladocopium* spp. symbionts. *P. damicornis* was selected due to its ecological relevance on Indo-Pacific reefs and its widespread use in experimental studies of coral-symbiont interactions and stress responses.

Coral bleaching

Coral branches (3 to 4 cm in length) were placed in a 50-liter tank illuminated by LED lamps (4200 K, 16 W) on a 12-hour photoperiod (0600 to 1800). Temperature was controlled using an Inkbird Temperature and Humidity Controller (Model ITC-608T) paired with a 500-W Titanium Aquarium Heater (Hygger, Model BUS-HG902-500W). Water flow was maintained with a Hygger Circulation and Wave Pump (792 GPH, Model HG017-4W). For the bleaching treatment, one tank underwent a 30-min stepwise +0.9°C temperature ramp from 28.3° to 34.4°C, followed by a 4-hour peak hold at 34.5°C, then a return to 27.6°C for 16 hours. The tank was illuminated by a single floodlight providing photosynthetically active radiation of 150 to 300 μmol m^{-2} s^{-1}. Coral branches remained in the bleaching tanks for 12 to 16 days until all visible symbiont coloration was lost. As the corals became increasingly pale (approximately day 10), they were shaded to reduce algal growth. Light levels during shading were not quantitatively measured. The floodlight was blocked, but corals remained exposed to indirect ambient room light during daylight hours. Once fully bleached, the corals were transferred to a separate holding tank maintained at 27.4°C with an identical setup. Bleached corals remained shaded in this tank until fragmentation for experimentation. All coral branches were bleached simultaneously in a single tank before fragmentation and assignment to subsequent experimental treatments (fig. S13). Bleached corals were fed four to five times per week, and fragmented corals were fed twice a week during the experiment, with identical feeding across all treatments. Feeding levels were likely elevated compared to natural reef conditions.

Experimental design

Corals were fragmented using diagonal cutting pliers (Milwaukee 6″ Diagonal Cutting Pliers) and affixed to ceramic plugs (Saricho Ceramic White Coraline Coral Frag Plugs 24 mm) using super glue [Bulk Reef Supply, 10 oz. (295.73 ml) Bottle BRS Extra Thick Gel Super Glue]. For contacting pairs, fragments were positioned to maximize contact area. In all experiments, “contact” refers to direct visible tissue-tissue contact between paired coral fragments. For “noncontact” pairs, fragments were affixed to the plug 5 to 7 mm apart. The separation distance was selected to prevent contact between the fragments when their polyps were extended while maintaining proximity. The fragment plugs for all experiments described below were then placed in an experimental 50-liter tank, maintained at 27.4°C with an identical setup to the bleaching and control tanks described above. All experiments and controls were conducted in the same tank.

Contact (n = 5) and noncontact (n = 5) coral pairs shown in Fig. 1 were maintained concurrently and arranged in adjacent rows of five plugs, with coral fragments trimmed to 1 to 1.5 cm in length. Larg-er coral fragments shown in fig. S1 were 2 to 3 cm in length. All coral pairs were imaged and monitored weekly over a 9-week period. For the separation experiment in Fig. 2, coral pairs were maintained in contact for 3 weeks, 2 weeks, 1 week, 5 days, 3 days, and 1 day (n = 2 per time duration). At the end of each contact period, the healthy corals were manually separated from the bleached coral and detached from the base and then immediately reaffixed to the same plug 5 to 7 mm from the bleached fragment. Coral pairs were imaged immediately before and immediately after separation. Two sequential sets of coral pairs were monitored for 9 weeks: The first set consisted of six pairs with contact durations of 1, 2, and 3 weeks with two pairs per duration and the second set consisted of six pairs with contact durations of 1, 3, and 5 days with two pairs per duration. All coral pairs were imaged and monitored weekly over a 9-week period. Coral pairs imaged using laser scanning microscopy in Fig. 2 were affixed to 2 × 1 LEGO bricks. Straight branches were selected for both healthy and bleached corals and arranged perpendicular to the edge of the flat, long face of the brick to minimize the distance between the objective lens and the coral fragment (fig. S14). The LEGO-mounted corals were temporarily affixed to coral plugs for added weight when not being imaged and were detached and reaffixed for each imaging session. The LEGO-mounted corals were maintained concurrently and arranged in a single row of four. All coral pairs (n = 4) had three bleached polyps and three healthy polyps imaged and monitored every 3 days over a 12-day period. Coral pairs of different genets (R-G, n = 3; G-R, n = 3) in Fig. 3 were maintained concurrently and arranged in adjacent rows of three. All coral pairs were imaged and monitored weekly over a 9-week period. For monitoring symbiont flow during recolonization in Fig. 4, coral pairs (n = 6) were maintained concurrently and arranged in adjacent rows of three plugs. All coral pairs were imaged and monitored weekly over a 5-week period. For the separation of recovering coral pairs to investigate the disruption of fused tissue bridges, coral pairs (n = 12) were maintained concurrently and arranged in adjacent rows of six plugs. All coral pairs were imaged and monitored weekly for 2 to 3 weeks. At the end of the contact period, coral pairs were manually separated. For determining whether tissue damage resulted from contact and separation alone (fig. S11), coral pairs (n = 6) were maintained in contact for 24 hours. All coral pairs were manually separated. For early-stage symbiont transfer dynamics (fig. S12), coral pairs (n = 6) were imaged every 12 hours over a 72-hour period and manually separated. All separated coral pairs were imaged immediately before and immediately after separation. We developed a three-dimensional (3D)–printed coral slider in which coral fragments were affixed to opposing sides of a movable platform, enabling controlled transition between contact and separation (fig. S15). STL files for the platform are available as a Zenodo record at DOI: https://doi.org/10.5281/zenodo.21128851. Design summaries for all experiments are provided in table S2.

Microscope images

Coral fragments were imaged weekly using a smartphone (iPhone 14) coupled to a LEICA S6D Trinocular Stereo Microscope illuminated with a Fiber-Lite Series 180 high-intensity illuminator set to level 8 intensity. The smartphone was mounted in a custom 3D-printed holder to ensure alignment of the camera lens and microscope eyepiece. Images were captured at 1.5× digital magnification in “Live Photo” mode with the stereomicroscope set to 0.63× magnification.

For coral pairs in contact, images were captured from three orientations: both lateral interface views and a frontal view of the bleached fragment. For coral pairs not in contact, the same three orientations were captured along with two views focused on the bleached fragment with the stereoscope set to 1.0× magnification. Noncontact pairs were imaged at 1× to 1.5× digital magnification, depending on fragment size and spacing. All fragments were removed from the water for imaging and returned immediately afterwards.

Polyp recovery

Polyp recovery in bleached fragments was assessed weekly. At week 0, after fragments were glued onto the plugs, the total number of visible polyps on each bleached fragment was recorded. Polyps at the contact interface and not visible were excluded. Individual polyps were recorded as recovered when symbiont repopulation was evident in all tentacles, appearing as a uniformly dark-brown ring. We only monitored polyps that were present at week 0; newly formed polyps during coral growth were not quantified, and skeletal growth rates were not measured in this study.

Image color analysis

Microscope images of coral pairs were manually segmented using MATLAB’s Image Processing Toolbox (Reference MALTAB R2024b) using the draw polygon function. Polygons were then converted to image masks using the poly2mask function, and median pixel red, green, and blue values were calculated. Pixel color distance between coral pairs was calculated as the Euclidean distance between the respective median pixel values in RGB space (Figs. 1E and 2D, and figs. S1E and S6E).

Area of algal overgrowth and overtake analysis

Algal overgrowth was estimated from the microscope images using the same polygon tracing methodology as above. Because of slight misalignments in the orientation of the coral at different time points, all algal overgrowth is reported as a fraction of the total visible coral surface (0 to 1), including dead regions of the fragment (Figs. 1D and 2C and figs. S1D and S6D). Area of healthy coral overgrowth in the mixed genet pairs was estimated from the microscope images following the methodology for the algal overgrowth (Fig. 3D).

LSCM images

Confocal imaging was performed using a Zeiss LSM980 equipped with an EC Plan-Neofluar 10×/0.30 M27 objective in Airyscan SR mode, controlled via Zeiss ZEN software. Coral fragments mounted on 2 by 1 LEGO bricks were placed on 22 by 50 mm no. 1 glass coverslips (Avantor VWR 48393-059) and maintained at room temperature (~18°C). For each coral pair, z-stacks spanning the full visible coral surface (30 to 100 µm, depending on the curvature of the coral fragment) were acquired from three polyps on both healthy and bleached fragments. The z-step size was 10 µm, ensuring individual symbionts were captured across at least two consecutive optical slices. Imaging was conducted in two fluorescence channels: chlorophyll-*a* autofluorescence (excitation 639 nm, laser power 0.20%, pinhole 5 AU) and GFP autofluorescence (excitation 488 nm, laser power 0.10%, pinhole 5.62 AU), both detected over 380 to 735 nm for both channels. Images were acquired at a pixel size of 2.368 µm using a GaAsP-PMT detector. To minimize stress, corals were not exposed to air for longer than 30 min, and repeated laser exposure was limited; these procedures, together with occasional grazing by invertebrates in the aquarium between time points, may have contributed to minor variation between imaging time points compared with corals imaged using stereoscopy.

LSCM image segmentation analysis

Z-stacks were processed in Fiji/ImageJ. For each stack, a maximum intensity projection was generated for both channels. The GFP channel was used to manually delineate the outer polyp boundary and inner polyp cavity, and a donut-shaped region of interest (ROI) was then generated by subtracting the inner boundary from the outer boundary, restricting analysis to only live coral polyp tissue. The resulting ROI was applied to the chlorophyll-*a* channel to isolate symbiont-associated autofluorescence. Images were then smoothed using a Gaussian filter (σ = 0.5) and thresholded to generate a binary mask, and small artifacts were removed before analysis. Symbionts were identified as local maxima within the masked tissue region using the Find Maxima function (noise threshold = 30). Symbiont counts were normalized to ROI area to calculate symbiont density per square millimeter. The quantified output was exported to a CSV summary file for downstream analysis in R. All ROI selections and intermediate images were archived for quality control. See fig. S16 for a visual representation of the image analysis pipeline.

Statistical analyses were performed in R (version 4.4.2). Symbiont density measurements from three polyps per fragment were averaged to generate a single fragment-level value, which was treated as the biological replicate (n = 4 fragments per condition). For comparisons of symbiont density between healthy and recovering fragments across time, fragment-level mean symbiont densities were calculated for each sampling day. Healthy and recovering fragments originating from a contacting pair were analyzed as paired biological replicates, where the number of symbionts in the recovering fragment was expressed as a percentage of the number of symbionts in the paired healthy fragment.

To quantify symbiont population doubling time, symbiont density of recovering fragments was analyzed separately during early (days 0 to 6) and late (days 6 to 12) recovery windows. For each fragment and time window, an exponential growth rate was estimated by fitting a linear model to log-transformed symbiont density as a function of time: $\log(N) = \log(N_0) + rt$, where N is symbiont density and r is the exponential growth rate. Doubling time was calculated as $t_\mathrm{d} = \ln(2)/r$. Models were fitted using fragment-level mean symbiont densities. For visualization, fitted model predictions were plotted on a logarithmic y axis together with observed symbiont densities. Mean doubling times are reported as mean ± SD across fragments, excluding cases with nonpositive growth rates.

Symbiont densities were quantified from the visible tissue surface and therefore may not fully capture variation in symbiont abundance throughout the entire tissue depth. As confocal imaging relies on light penetration, fluorescence from deeper tissue layers may be obscured by tissue opacity and light scattering, potentially leading to underestimation of symbiont densities. In addition, in regions of high symbiont density, closely adjacent cells may not be resolved as separate local maxima during image analysis, which could further underestimate symbiont density. However, because all coral fragments were imaged and analyzed using identical acquisition and quantification parameters, these limitations are unlikely to affect comparisons between conditions over time.

Acknowledgments

We thank the Stanford SuperReefs Project for support. We thank G. Donahue for coral husbandry and tank maintenance. We thank all the members of the Micheli and Palumbi laboratories for helpful discussions and advice throughout the course of this study.

Funding:

This work was supported by National Science Foundation grant no. 2412742 (S.R.P.), National Science Foundation grant no. 2108566 (F.M.), the Knight-Hennessy Scholars Program at Stanford University (D.S.C.), Start-up funds from Stanford University (V.B.), and a Seed grant from MAC3 Impact Philanthropies and Stanford Woods Institute for the Environment (S.R.P.)

Author contributions:

Conceptualization: D.S.C., F.M., and S.R.P. Methodology: D.S.C., J.S., T.R., C.N.K., V.B., F.M., and S.R.P. Software: D.S.C., J.S., and N.R.M. Validation: D.S.C. and J.S. Formal analysis: D.S.C., J.S., and N.R.M. Investigation: D.S.C. and J.S. Resources: D.S.C., J.S., N.R.M., V.B., F.M., and S.R.P. Data curation: D.S.C., J.S., and N.R.M. Writing—original draft: D.S.C., J.S., N.R.M., F.M., and S.R.P. Writing—review and editing: All authors. Visualization: D.S.C., J.S., N.R.M., G.F.C., and S.R.P. Supervision: F.M. and S.R.P. Project administration: D.S.C., F.M., and S.R.P. Funding acquisition: F.M., S.R.P., and V.B.

Competing interests:

The authors declare that they have no competing interests.

Data, code, and materials availability:

All data and code needed to evaluate and reproduce the results in the paper are present in the paper and/or the Supplementary Materials. Analyses were performed using MATLAB R2024b (Image Processing Toolbox) and Fiji (ImageJ). Data are available as a Zenodo record (DOI: https://doi.org/10.5281/zenodo.21128851). This study did not generate new code. This study did not generate new materials.

Supplementary Materials

The PDF file includes:

Figs. S1 to S16

Tables S1 and S2

Legend for movie S1

Download, PDF (31.61 MB)

Other Supplementary Material for this manuscript includes the following:

Movie S1

Download, ZIP (47.30 MB)

REFERENCES

1 T. P. Hughes, J. T. Kerry, M. Álvarez-Noriega, J. G. Álvarez-Romero, K. D. Anderson, A. H. Baird, R. C. Babcock, M. Beger, D. R. Bellwood, R. Berkelmans, T. C. Bridge, I. R. Butler, M. Byrne, N. E. Cantin, S. Comeau, S. R. Connolly, G. S. Cumming, S. J. Dalton, G. Diaz-Pulido, C. M. Eakin, W. F. Figueira, J. P. Gilmour, H. B. Harrison, S. F. Heron, A. S. Hoey, J.-P. A. Hobbs, M. O. Hoogenboom, E. V. Kennedy, C. Kuo, J. M. Lough, R. J. Lowe, G. Liu, M. T. McCulloch, H. A. Malcolm, M. J. McWilliam, J. M.

Pandolfi, R. J. Pears, M. S. Pratchett, V. Schoepf, T. Simpson, W. J. Skirving, B. Sommer, G. Torda, D. R. Wachenfeld, B. L. Willis, S. K. Wilson, Global warming and recurrent mass bleaching of corals. *Nature* **543**, 373–377 (2017).

+ SEE ALL REFERENCES • CROSSREF • PUBMED • WEB OF SCIENCE • GOOGLE SCHOLAR

2 R. D. Gates, G. Baghdasarian, L. Muscatine, Temperature stress causes host cell detachment in symbiotic cnidarians: Implications for coral bleaching. *Biol. Bull.* **182**, 324–332 (1992).

GO TO REFERENCE • CROSSREF • PUBMED • WEB OF SCIENCE • GOOGLE SCHOLAR

SHOW ALL REFERENCES

eLetters (0)

eLetters is a forum for ongoing peer review. eLetters are not edited, proofread, or indexed, but they are screened. eLetters should provide substantive and scholarly commentary on the article. Neither embedded figures nor equations with special characters can be submitted, and we discourage the use of figures and equations within eLetters in general. If a figure or equation is essential, please include within the text of the eLetter a link to the figure, equation, or full text with special characters at a public repository with versioning, such as Zenodo. Please read our Terms of Service before submitting an eLetter.

LOG IN TO SUBMIT A RESPONSE

No eLetters have been published for this article yet.

Recommended articles from TrendMD

Symbioses are restructured by repeated mass coral bleaching
Kate M. Quigley, Sci Adv, 2022

The Acquisition of Exogenous Algal Symbionts by an Octocoral After Bleaching
Cynthia L. Lewis, Science, 2004

Single Symbionts for Corals
Science, 2006

Climate change disables coral bleaching protection on the Great Barrier Reef
Tracy D. Ainsworth, Science, 2016

Trophic strategy and bleaching resistance in reef-building corals
Inga E. Conti-Jerpe, Sci Adv, 2020

Powered by MD

CURRENT ISSUE

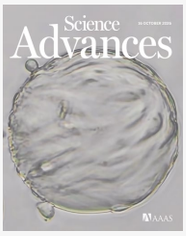

Mitochondrial carbonic anhydrase–VB inhibition rescues brain endothelial stress and memory in Alzheimer's disease models
BY NICOLE L. LEMON, ELISA CANEPA, *ET AL.*

How inequality became durable before states: Evidence from 6000 years in the Central Plain of China
BY DONGDONG LI, SUWEI GUO, *ET AL.*

Macrophage- or neutrophil-expressed UPP1 drives tumor growth and immune suppression in the tumor microenvironment
BY YIN LI, QIN RAN, *ET AL.*

TABLE OF CONTENTS

ADVERTISEMENT

Sign up for ScienceAdviser

Get *Science*'s award-winning newsletter with the latest news, commentary, and research, free to your inbox daily.

SUBSCRIBE

LATEST NEWS

ADVERTISEMENT

SCIENCEINSIDER | 14 OCT 2026

NSF backs choice of new Antarctic contractor despite concerns by government watchdog and researchers

NEWS | 14 OCT 2026

Coral can heal rapidly from bleaching—if it touches a clone

NEWS | 14 OCT 2026

Can predictive tools tell us who really needs antidepressants?

SCIENCEINSIDER | 14 OCT 2026

Mountaintop microwave observatory will peer into the infant universe

NEWS | 13 OCT 2026

This year's 'super' El Niño could wreak ecological havoc worldwide

SCIENCEINSIDER | 13 OCT 2026

AI edges closer to solving the Riemann hypothesis, one of math's hardest problems

ADVERTISEMENT

RELATED JOBS

Assistant, Associate, Full Professor (Tenured or Tenure Track)

University of Wisconsin-Madison, Department of Biochemistry
Madison, Wisconsin

Postdoctoral and Predoctoral Fellow Positions

Unversity of Illinois at Chicago
Chicago, Illinois

Tenure-Track Assistant Professor Faculty Position

Vanderbilt University
Nashville, Tennessee

MORE JOBS ▶

RECOMMENDED

PERSPECTIVE | APRIL 2013

Dynamics of Coral Reef Recovery

8 APR 2020 | BY JEFFREY BRAINARD

Great Barrier Reef experiences massive coral bleaching

RESEARCH NEWS | NOVEMBER 1987

Coral Bleaching Threatens Atlantic Reefs

REPORT | APRIL 2013

Recovery of an Isolated Coral Reef System Following Severe Disturbance

SPONSORED WEBINAR | TECHNOLOGY | 21 OCT 2026

Battle for the gut: From microbial competition to therapeutic communities

FOLLOW US

GET OUR NEWSLETTER

NEWS
All News
ScienceInsider
News Features
Subscribe to News from Science
News from Science FAQ
About News from Science
Donate to News

CAREERS
Careers Articles
Find Jobs
Employer Hubs

COMMENTARY
Opinion
Analysis
Blogs

JOURNALS
Science
Science Advances
Science Immunology
Science Robotics
Science Signaling
Science Translational Medicine
Science Partner Journals

AUTHORS & REVIEWERS
Information for Authors
Information for Reviewers

LIBRARIANS
Manage Your Institutional Subscription
Library Admin Portal
Request a Quote
Librarian FAQs

ADVERTISERS
Advertising Kits
Custom Publishing Info
Post a Job

RELATED SITES
AAAS.org
AAAS Communities
EurekAlert!
Science in the Classroom

ABOUT US
Leadership
Work at AAAS
Prizes and Awards

HELP
FAQs
Access and Subscriptions
Order a Single Issue
Reprints and Permissions
TOC Alerts and RSS Feeds
Contact Us

© 2026 American Association for the Advancement of Science. All rights reserved. AAAS is a partner of HINARI, AGORA, OARE, CHORUS, CLOCKSS, CrossRef and COUNTER. *Science Advances* eISSN 2375-2548.

Terms of Service | Privacy Policy | Cookie Preferences | Accessibility